

Spatial oscillations in strain fields due to paraelastic defects

B. G. Dick

University of Utah, Salt Lake City, Utah 84112

(Received 8 October 1980)

Analytic expressions based on a phonon rather than an elastic continuum treatment are given for lattice relaxation displacements and strains in the vicinity of paraelastic defects in cubic crystals. Relaxation energies are also given in closed form. The approximations involved in deriving these results are the use of the long-wave strain limiting form of the defect-phonon interaction and the use of a Debye model for the phonons as well as a modified Debye model with appropriate Van Hove singularity at the Debye cutoff. The elastic continuum limit in which the Debye frequency is allowed to go to infinity is investigated. Only the modified Debye model gives sensible results in this limit. The analytic expressions can be evaluated in terms of host-crystal parameters and measured stress-coupling parameters of the defect. Displacements and energies are calculated for nine different defect systems. It is found that the modified Debye model predicts defect interactions which are of longer range than does the elastic continuum model and that these interactions show a spatially oscillatory character at large defect separations.

Because of their strong interaction with their host lattice, molecular and off-center defects in alkali halide crystals exhibit small polaronlike properties.¹⁻⁶ Among these properties is the renormalization of tunneling matrix elements connecting equivalent orientations of the defect. This renormalization is due to reduction of phonon harmonic oscillator wave functions because of lattice relaxation displacements of ions near the defect. This effect is conveniently treated by means of the polaron transformation which eliminates from the defect-lattice Hamiltonian that defect-phonon interaction term linear in lattice displacements by means of a unitary transformation.⁷ This same transformation applied to the lattice displacement operators yields expressions for the associated static lattice displacements in the vicinity of the defect. Such displacements give rise to electric field gradients in the defect region which could in principle be detected by their interactions with nuclear electric quadrupoles, although we do not concern ourselves with this aspect of the relaxation here.

In this paper approximate expressions for these displacements are derived in analytic form. The approximations involved are (1) the use of the simplest form of the defect-phonon interaction, the long-wave strain limiting form, and (2) the use of a Debye model for the phonons. A modified form of the Debye model, in which the appropriate Van Hove singularity at the maximum phonon frequency is introduced, is also investigated to give some idea of

the sensitivity of our results to the assumed form of the phonon spectrum. It is found that the use of this modified Debye model is essential in achieving a sensible expression for the volume change associated with the A_{1g} distortion created by the defect. The resulting expressions for the lattice displacements, although of course approximate, are easily evaluated in terms of tabulated functions and depend only on readily measurable quantities associated with the defect and the host crystal. It is found that the displacements are not too sensitive to the form of the phonon spectrum (within the limitations of the models tried) suggesting that the approximate nature of the calculation might not be too drastic. Using the Debye model is, of course, not the same as using elastic continuum theory because of the finite maximum Debye frequency. Elastic continuum theory results follow from the modified Debye model results given here by taking the limit $\tilde{\omega}_D \rightarrow \infty$.

The analytic expressions for lattice displacements can be differentiated to give expressions for elastic strain components which can be used to study paraelastic defect interactions. It is found that the strains have an oscillatory character reminiscent of Friedel oscillations of the screening of a charge defect in a metal. A consequence of these oscillations is a longer range for defect interactions than that predicted on the basis of elastic continuum theory.

In Sec. II expressions for lattice displacements created by a [100] elastic dipole defect system are

derived for both Debye and modified Debye models. Section III gives analogous results for [111] and [110] elastic dipole systems. Section IV gives relaxation energy expressions and Sec. V presents some numerical results for displacements and energies. Section VI discusses strains produced by elastic dipoles and the interaction of paraelastic defects. An appendix outlines the evaluation of certain integrals occurring in the modified Debye model.

II. METHOD AND [100] DEFECTS

In Ref. 3, Eq. (36), it is shown that the α Cartesian component of the displacement of the lattice site occupant at L due to a defect with orientation i is given by

$$\delta_i X_{L\alpha} = \left(\frac{2}{\hbar} \right)^{1/2} \sum_f \chi \left[\begin{matrix} L \\ \alpha \\ f \end{matrix} \right] D_f^i \omega_f^{-3/2}. \quad (1)$$

Here the sum over f is over the phonon modes, the D_f^i are coefficients appearing in the linear defect-phonon operator [Ref. 3, Eqs. (25) and (31)]. The superscript i on χ in (1) above, which appears in Ref. 3 has been omitted here since we are omitting the quadratic defect-phonon interaction term.

For the D_f^i we will use the so-called long-wave limiting form in which the phonon-defect interaction arises exclusively from the strain produced by the phonons. For [100]-, [111]-, and [110]-oriented defects the coupling to strain is given by

$$H_s([100]) = -\frac{1}{3}\gamma_1(2e_{xx} - e_{yy} - e_{zz}), \quad (2)$$

$$H_s([111]) = -\frac{3}{4}\gamma_2(e_{xy} + e_{yz} + e_{zx}), \quad (3)$$

$$D_f^{100} = -(i/3)\gamma_1(\hbar/2\omega_f M_c)^{1/2}[2e_x(j)q_x - e_y(j)q_y - e_z(j)q_z], \quad (8)$$

$$D_f^{111} = -(3i/4)\gamma_2(\hbar/2\omega_f M_c)^{1/2}[e_x(j)q_y + e_y(j)q_x + \text{c.p.}], \quad (9)$$

$$D_f^{110} = i(\hbar/2\omega_f M_c)^{1/2} \left\{ \frac{1}{3}\gamma_1[2e_z(j)q_z - e_x(j)q_x - e_y(j)q_y] - \frac{3}{2}\gamma_2[e_x(j)q_y + e_y(j)q_x] \right\}, \quad (10)$$

$$D_f^{A_{1g}} = i\gamma_0(\hbar/2\omega_f M_c)^{1/2}[e_x(j)q_x + e_y(j)q_y + e_z(j)q_z], \quad (11)$$

where c.p. is a cyclic permutation.

If the long-wave limiting form of the defect-phonon interaction were abandoned in favor of an interaction which is linear in the displacements of neighbors nearest to the defect (and not just the strain at the defect site), then the q_i factors in (8)–(11) would be replaced by $(\sin q_i a)/a$. For the sake of the analytic results of this paper we have not used this “linear in displacements” interaction. The

$$H_s([110]) = -\frac{1}{3}\gamma_1(2e_{zz} - e_{xx} - e_{yy}) - \frac{3}{2}\gamma_2 e_{xy}, \quad (4)$$

where $\gamma_1 = \alpha_1(c_{11} - c_{12})$ and $\gamma_2 = \alpha_2 c_{44}$, α_1 and α_2 being the stress parameters as defined in the tabulation of Bridges.⁸ The c_{ij} are the host-lattice elastic stiffness constants which we assume to be unaltered by the defect. The interactions (2)–(4) have been constructed so that the sum over defect orientations vanishes and consequently omits the A_{1g} distortion due to the defect. For the purpose of investigating lattice displacements this A_{1g} part should be restored. It has the form

$$H_s(A_{1g}) = \gamma_0(e_{xx} + e_{yy} + e_{zz}), \quad (5)$$

and will be treated separately later.

Since the displacement operator is given by

$$X_{L\alpha} = \sum_f \chi \left[\begin{matrix} L \\ \alpha \\ f \end{matrix} \right] i \left(\frac{\hbar}{2\omega_f} \right)^{1/2} (a_f - a_f^\dagger), \quad (6)$$

where

$$\chi \left[\begin{matrix} L \\ \alpha \\ f \end{matrix} \right] = (M_c)^{-1/2} e_\alpha(j) \exp[i\vec{q} \cdot \vec{X}(L)] \quad (7)$$

for Debye phonons [see Ref. 4, Eq. (22)], the strains produced by phonons at the origin of coordinates (where we assume the defect to be situated) can be written in terms of phonon creation and annihilation operators: The strain components are derivatives of (6) evaluated at the origin. Comparing with Ref. 3, Eq. (31) we find

$\vec{e}(j)$ are phonon eigenvectors for mode j , the q_i phonon wave numbers, and M_c is the crystal mass.

In the Debye approximation

$$\sum_f \rightarrow \frac{V}{2\pi^2} \int_0^{\omega_D} \omega^2 d\omega \sum_j c_j^{-3} \int \frac{d\Omega}{4\pi}, \quad (12)$$

the j sum being over two transverse and one longi-

tudinal wave with wave velocities c_j . We will also consider (and be forced to opt for) a modified Debye model⁹ in which the integral over ω in (12) is replaced by

$$\int_0^{\tilde{\omega}_D} \omega^2 \left[1 - \left(\frac{\omega}{\tilde{\omega}_D} \right)^2 \right]^{1/2} d\omega. \quad (13)$$

This has the appropriate Van Hove singularity at $\tilde{\omega}_D$. In order that the total number of degrees of freedom be the same both the Debye and modified Debye models it is required that

$$\hat{q} = \vec{e}(l) = (Asx + BFsy + BEc, -Bsx + AFsy + AEc, -Esy + Fc), \quad (14)$$

$$\vec{e}(t_1) = (Ay - BFx, -By - AFx, Ex), \quad (15)$$

$$\vec{e}(t_2) = (Acx + BFcy - BEs, -Bcx + AFcy - AEs, -Ecy - Fs). \quad (16)$$

For conciseness we have used the notation $A = \sin\Phi$, $B = \cos\Phi$, $E = \sin\Theta$, $F = \cos\Theta$, $x = \sin\phi$, $y = \cos\phi$, $s = \sin\theta$, and $c = \cos\theta$. Using $\vec{q} = \omega\hat{q}/c_j$ and performing the ϕ integration in (1) with (12), many terms vanish. The initial algebraic step in this process is tedious. In the case of [110] defects, for example, it involves consideration of 850 terms. The labor was much diminished by use of the algebraic programming system REDUCE.¹⁰ The surviving θ integrations, having chosen the real part of (1), can be reduced to two types

$$I_1(a_j) = \int_0^\pi d\theta \sin^3\theta \cos\theta \sin(a_j \cos\theta) = \frac{4j_2(a_j)}{a_j}, \quad (17)$$

$$I_2(a_j) = \int_0^\pi d\theta \sin\theta \cos\theta \sin(a_j \cos\theta) = 2j_1(a_j), \quad (18)$$

$$\delta_{100}X_{Lx} = (A_{100}/R^2)[3(3 - 5\xi^2)(\Lambda_1^l - \Lambda_1^t) + 2(3\xi^2 - 1)\Lambda_2^l + 6(1 - \xi^2)\Lambda_2^t]\xi, \quad (22)$$

$$\delta_{100}X_{Ly} = (A_{100}/R^2)[3(1 - 5\xi^2)(\Lambda_1^l - \Lambda_1^t) + 2(3\xi^2 - 1)\Lambda_2^l - 6\xi^2\Lambda_2^t]\eta, \quad (23)$$

$$\delta_{100}X_{Lz} = (A_{100}/R^2)[3(1 - 5\xi^2)(\Lambda_1^l - \Lambda_1^t) + 2(3\xi^2 - 1)\Lambda_2^l - 6\xi^2\Lambda_2^t]\xi, \quad (24)$$

where $A_{100} = \gamma_1/12\pi^2\rho$. ξ , η , and ξ are the direction cosines of \vec{L} . This E_g distortion of the lattice has the necessary property $\int \delta_{100}\vec{X} \cdot d\vec{A} = 0$, the integral being taken over a spherical surface centered at the origin. Thus there is no net volume change associated with the E_g distortion. The diminishing oscillations exhibited by the asymptotic forms in (20) and (21) are reminiscent of the Friedel oscilla-

$\tilde{\omega}_D = \omega_D(16/3\pi)^{1/3}$. To be consistent with our simple model we use the elementary Debye model result $\omega_D^3 = 6\pi^2\bar{c}^3/a^3$ where a is the host-crystal nearest-neighbor distance and $1/\bar{c}^3 = (2c_t^{-3} + c_l^{-3})/3$.

To perform the integrations in (1) we write the lattice site position vector \vec{L} in terms of spherical polar coordinates R, Θ, Φ with the crystallographic z axis as the polar axis. So as to simplify $\vec{q} \cdot \vec{L}$ ($= qR \cos\theta$), the q and $e(j)$ vectors are then written in terms of spherical polar coordinates θ, ϕ with L chosen as the polar axis:

where j_1 and j_2 are spherical Bessel functions and $a_j = R\omega/c_j$.

The remaining integrations over ω are straightforward in the Debye case:

$$\int_0^{\omega_D} \omega d\omega I_i(a_j) = \left[\frac{2c_j^2}{R^2} \right] K_i(g_j), \quad (19)$$

where $g_j = R\omega/c_j$,

$$K_1(g) = \text{Si}(g) - 3j_1(g) \sim \frac{1}{2}\pi + 2\text{csc}g/g, \quad (20)$$

$$K_2(g) = \text{Si}(g) - \text{sing} \sim \frac{1}{2}\pi - \text{sing} - \text{csc}g/g. \quad (21)$$

Since $\bar{c}^3 \simeq 3c_t^3/2$, $g_j \simeq (9\pi)^{1/3} (R/a)(c_t/c_j)$. The asymptotic forms are those for large g (R greater than a few nearest-neighbor distances). Defining $\Lambda_i^j = c_j^{-2}K_i(g_j)$, the three components of the non- $A_{1g}(E_g)$ displacement of an ion at R, Θ, Φ are given by

tions¹¹ in the screening of a point charge in an electron gas. The occurrence of Λ_i^l and Λ_i^t each with its own length scale in its argument is an artifact of our modified Debye spectrum which fixes a single cutoff frequency ω_D . This produces two different cutoff q vectors which lead to the two length scales. Because of the c_j^{-2} factors in the definition of the Λ_i^j and because $c_t^2/c_l^2 = c_{44}/c_{11}$, the Λ_i^l are typically

only about 15% as large as the Λ_i^l . We will occasionally omit Λ_i^l terms in the following discussion.

By the same method one finds the radial A_{1g} displacements to have the magnitude

$$\delta_{A_{1g}} X = -(\gamma_0/2\pi^2\rho R^2)\Lambda_2^l. \quad (25)$$

Paus and Lüty¹² have measured $\Delta V/V$ for KCl:OH⁻ and found it to be -0.21 per defect. The asymptotic form of Λ_2^l for large R is $(\frac{1}{2}\pi - \text{sing}_l)/c_l^2$. Using this, one ought to be able to relate γ_0 to this measured $\Delta V/V$ through

$$\begin{aligned} \frac{\Delta V}{V} &= a^{-3} \int \delta_{A_{1g}} \vec{X} \cdot d\vec{A} \\ &= -\frac{\gamma_0}{c_{11}a^3} \left[1 - \frac{2}{\pi} \sin \left[\frac{R\omega_D}{c_l} \right] \right], \end{aligned} \quad (26)$$

$$\begin{aligned} \tilde{K}_1(g) &= \frac{1}{2}\pi \{ gJ_0(g) - J_1(g) + \frac{1}{2}\pi(g - 3g^{-1})[J_1(g)H_0(g) - J_0(g)H_1(g)] \} \\ &\sim \frac{1}{2}\pi + (\sqrt{2\pi/g^{3/2}})\cos(g - \frac{1}{4}\pi), \end{aligned} \quad (28)$$

$$\begin{aligned} \tilde{K}_2(g) &= \frac{1}{2}\pi \{ gJ_0(g) - 2J_1(g) + \frac{1}{2}\pi g[J_1(g)H_0(g) - J_0(g)H_1(g)] \} \\ &\sim \frac{1}{2}\pi - \sqrt{\pi/2g} \cos(g - \frac{3}{4}\pi). \end{aligned} \quad (29)$$

Here the J_n 's are Bessel functions and the H_n 's are Struve functions. An outline of the evaluation of these integrals is given in the Appendix. \tilde{K}_1 and \tilde{K}_2 are plotted as a function of g in Fig. 1.

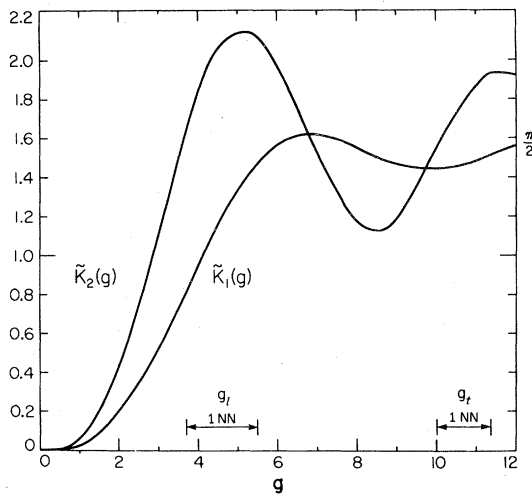


FIG. 1. The functions $\tilde{K}_1(g)$ and $\tilde{K}_2(g)$ defined in Eqs. (28) and (29). The range of g values g_l and g_r for the first-nearest-neighbor distances of the systems discussed in Sec. V are shown.

but the sine term would imply that $\Delta V/V$ is a very sensitive function of crystal size and appears to be spurious. Indeed it is; this oscillating term in the surface integral is an artifact of the incorrect sharp cutoff of the Debye spectrum (which must be abandoned in favor of the modified Debye model).

This can be seen by carrying out the calculations using the modified Debye density of states (13). For this case the integrals (19) become

$$\int_0^{\tilde{\omega}_D} d\omega \omega \left[1 - \left[\frac{\omega}{\tilde{\omega}_D} \right]^2 \right]^{1/2} I_i(a_j) = \left[\frac{2c_j^2}{R^2} \right] \tilde{K}_i(\tilde{g}_j), \quad (27)$$

with $\tilde{g}_j = \tilde{\omega}_D R/c_j$. The displacements in the modified Debye case are given by (22)–(24) with the K 's replaced by \tilde{K} 's. These integrals, like (20) and (21), can also be expressed in terms of tabulated functions:

Note that the leading terms in the asymptotic forms of \tilde{K}_1 and \tilde{K}_2 are the same as those for K_1 and K_2 . This is to be expected since the modified Debye spectrum does not alter the density of the long-wave phonons which determine the displacements for large R . Note also that the oscillating parts of the modified Debye asymptotic forms fall off more rapidly for large R (with an extra factor of $R^{-1/2}$) than for the Debye case but they are not eliminated by modifying the abrupt Debye cutoff. We note from (29) that the bothersome oscillating term in (26) is absent when the modified Debye spectrum is used and $\Delta V/V = -\gamma_0/c_{11}a^3$, an expression which unlike (26) is independent of crystal size. It is also independent of $\tilde{\omega}_D$ and hence unchanged by going to the elastic continuum limit. This is, in fact, the elastic continuum theory result of Nowick and Heller.¹³

Using Lighthill's¹⁴ method of finding asymptotic forms of Fourier integrals one can readily deduce the asymptotic expressions in (28) and (29) without having to evaluate the integrals. This procedure is interesting because it shows that the constant asymptotic terms in (28) and (29) are governed entirely by the phonon spectrum near $\omega = 0$ while the

oscillating terms are produced by the form of the Van Hove singularity at $\tilde{\omega}_D$. These particular features of the phonon spectrum are not mere artifacts of the modified Debye model but are quite general requirements of any adequate phonon spectrum.¹⁵ Furthermore, the use of the long-wave limiting form of the defect-phonon interaction does not seem to be an artificiality which itself produces the unusual asymptotic displacement fields. In a more elaborate model using summations over actual phonons and a more accurate form of the D_f^j such as that discussed under (11) above, one might worry that the $(\text{sing}_i a)$ factors might vanish at the

Brillouin-zone boundary where the Van Hove singularities of primary interest to us occur. This would lead to a vanishing of the coupling of the defect to zone-edge phonons and a suppression of the role of the associated Van Hove singularities. This occurs only at a few points on the zone boundary surface (e.g., the point X) and is not in general the case. Thus, the asymptotic forms of (28) and (29) have a more general validity than our approximate method derivation might imply. We do not here investigate the possible contributions to asymptotic displacement fields from Van Hove singularities other than those at $\omega = 0$ and $\omega = \tilde{\omega}_D$.

III. [111] AND [110] DEFECTS

Using the methods of Sec. II and Eqs. (3) and (4) one can deduce non- A_{1g} displacement expressions for [111] and [110] defects. For a [111] defect the T_{2g} displacements are given by

$$\delta_{111}X_{Lx} = (A_{111}/R^2)\{ [2(\Lambda_2^t - \Lambda_2^i) - 5(\Lambda_1^t - \Lambda_1^i)](\xi\eta + \eta\xi + \zeta\xi)\xi + (\Lambda_1^t - \Lambda_1^i + \Lambda_2^t)(\eta + \xi) \}, \quad (30)$$

with $\delta_{111}X_{Ly}$ and $\delta_{111}X_{Lz}$ being given by cyclic permutations of the direction cosines ξ, η, ζ , in (30). Here $A_{111} = 3\gamma_2/8\pi^2\rho$.

For a [110] defect the displacements (both E_g and T_{2g}) are given by

$$\delta_{110}X_{Lx} = (A_{110}/R^2)[3(\Lambda_1^t - \Lambda_1^i)(1 - 5\xi^2) + 2\Lambda_2^t(1 - 3\xi^2) + 6\Lambda_2^t\xi^2]\xi + (B_{110}/R^2)[(\Lambda_1^t - \Lambda_1^i)(5\xi^2 - 1) + 2\Lambda_2^t\xi^2 + \Lambda_2^t(1 - 2\xi^2)]\xi, \quad (31)$$

$$\delta_{110}X_{Lz} = (A_{110}/R^2)[3(\Lambda_1^t - \Lambda_1^i)(3 - 5\xi^2) + 2\Lambda_2^t(1 - 3\xi^2) - 6\Lambda_2^t(1 - \xi^2)]\xi + (B_{110}/R^2)[5(\Lambda_1^t - \Lambda_1^i) + 2(\Lambda_2^t - \Lambda_2^i)]\xi\eta\xi, \quad (32)$$

and $\delta_{110}X_{Ly}$ is the same as (31) with ξ and η interchanged, where $A_{110} = \gamma_1/12\pi^2\rho$ and $B_{110} = 3\gamma_2/4\pi^2\rho$. As with the [100] case, in both the [111] and [110] defect cases, the modified Debye forms of the displacements follow from expressions (20)–(32) with Λ_i^j replaced by $\tilde{\Lambda}_i^j$. It can be readily verified that there is no net volume change associated with these non- A_{1g} distortions. In (22)–(24) and (30)–(32) the elastic continuum results follow if one takes $\tilde{\omega}_D \rightarrow \infty$. This causes $\tilde{\Lambda}_i^j \rightarrow \pi/2c_j^2$ throughout. Note that only the modified Debye model yields a sensible elastic continuum limit.

IV. ENERGIES OF RELAXATION

The energy associated with the polaronlike relaxation is given by

$$E = \sum_f \frac{|D_f|^2}{\hbar\omega_f} \quad (33)$$

according to Ref. 3, Eq. (37). E can be readily evaluated by the methods of Sec. II to give

$$\begin{aligned} E_{100} &= A \frac{2}{3}\gamma_1^2, \\ E_{111} &= A \frac{9}{32}\gamma_2^2, \\ E_{110} &= A \left(\frac{2}{3}\gamma_1^2 + \frac{9}{4}\gamma_2^2 \right), \\ E_{A_{1g}} &= B\gamma_0^2, \end{aligned} \quad (34)$$

where

$$\begin{aligned} A &= \frac{1}{10\rho a^3} \left[\frac{3\beta^5 + 2}{2\beta^3 + 1} \right] \frac{1}{c_l^2}, \\ B &= 3/[2\rho a^3(2\beta^3 + 1)c_l^2], \end{aligned} \quad (35)$$

with $\beta = c_l/c_t$. These results are the same for both the Debye and modified Debye phonon spectra being independent of ω_D .

Since the defect-lattice interaction has been treated as arising solely from the strain produced by the defect, these energies include no electrostatic contribution.

V. NUMERICAL RESULTS — DISPLACEMENTS AND ENERGIES

To calculate relaxation displacements and energies by the methods of the previous sections we need

the measured defect stress parameters α_1 and/or α_2 along with the fractional volume change $\Delta V/V$ associated with the defect. Also needed are the host interionic distance, elastic constants, and density. The Struve functions which occur in (28) and (29) can be calculated using the Chebyshev polynomial method of Luke.¹⁶

Table I shows, for the case of the [100] defect KCl:OH⁻, displacements for the first five neighbors nearest to the defect and relaxation energies for the E_g and for the A_{1g} distortions. Results are shown for room-temperature and for 80 K elastic constants as well as for the Debye and modified Debye phonon spectra. The Paus and Lüty¹² value of -0.21 for $\Delta V/V$ and the stress parameter $\alpha_1 = 5.8 \times 10^{-24} \text{ cm}^3$ from Ref. 8 have been used. It is to be noted that the variation of displacements with choice of phonon spectrum is relatively slight except for the 111 neighbor in the case of the E_g distortion. A much larger change is produced by using 80 K instead of room-temperature elastic constants. Note that, at least for the case of KCl:OH⁻, the A_{1g} displacements and relaxation energies are an order of magnitude smaller than those associated with the E_g distortions. The oddity of slightly larger A_{1g} radial displacements for 200 neighbors than for 100 neighbors occurs in this model calculation because of an initial marked increase in $K_2(g)$ for small and increasing g .

Stress parameters for a number of other molecular or off-center defects have been tabulated by Bridges.⁸ Unfortunately, neither $\Delta V/V$ for any de-

fect system other than KCl:OH⁻ nor low-temperature elastic constants for host crystals other than KCl and KBr seem to have been measured. Table II shows calculated displacements and relaxation energies for these other systems. The stress parameters (in units 10^{-24} cm^3) used were the following. For the [100] systems KBr:OH⁻, RbCl:OH⁻, RbBr:OH⁻, RbI:OH⁻ $\alpha_1 = 7.68, 4.97, 8.67, 12.0$, respectively. For the [110] systems NaBr:F⁻, RbCl:Ag⁺, RbBr:Ag⁺ (α_1, α_2) = (2.12, 0.728), (7.42, 1.82), (13.7, 3.51). For the [111] system KCl:Li⁺ $\alpha_2 = 3.31$. For KCl:Li⁺ and for KBr:OH⁻ the results are given for both room-temperature and low-temperature elastic constants. Elastic constants have been taken from the tabulation of Huntington.¹⁷ The use of low-temperature rather than room-temperature elastic constants is seen to make little difference in the case of the [111] system KCl:Li⁺ while in the case of [100] KBr:OH⁻ mainly the 100 displacements and the relaxation energy are affected by this choice of elastic constants. It is interesting to note the small displacements and relaxation energy of the KCl:Li⁺ system compared with the other non-[111] systems. The 111 neighbor displacements are the only ones showing marked sensitivity to the form of the phonon spectrum, even changing sign with change from the Debye to the modified Debye forms in the case of NaBr:F⁻. The asymptotic identity of the Debye and modified Debye model displacement magnitudes appears to have been nearly achieved at fifth nearest neighbor distances.

TABLE I. Displacements for various neighbors and relaxation energies for the [100] KCl:OH⁻ system. RT (room temperature) or 80 K refer to the temperature at which the elastic constants were measured. E_g or A_{1g} refer to the symmetry of the distortion and D and MD refer to the choice of phonon spectrum: Debye or modified Debye. All displacements are given in hundredths of an angstrom. The column labels lmn refer to near-neighbor positions. The numbers in parentheses are the $x, y,$ and z components of the displacements. The E_g displacements at 0 ± 10 and 00 ± 1 sites are directed radially inward toward the defect and have magnitude half that shown for the 100 site.

Case			Site					E (eV)
			100	110	111	200	210	
RT	E_g	D	(26,0,0)	(1.7,3.8,0)	(-1.8,0.90,0.90)	(5.6,0,0)	(3.4,0.41,0)	0.12
RT	E_g	MD	(23,0,0)	(1.7,2.8,0)	(-0.2,0.11,0.11)	(6.0,0,0)	(3.5,0.9,0)	0.12
80 K	E_g	D	(31,0,0)	(1.9,4.5,0)	(-2.2,1.1,1.1)	(6.6,0,0)	(4.0,0.53,0)	0.18
80 K	E_g	MD	(27,0,0)	(1.8,3.5,0)	(-0.31,0.16,0.16)	(7.1,0,0)	(4.1,1.1,0)	0.18
RT	A_{1g}	D	(-1.6,0,0)	(-1.4,-1.4,0)	(-1.1,-1.1,-1.1)	(-1.8,0,0)	(-1.5,-0.74,0)	0.016
RT	A_{1g}	MD	(-1.6,0,0)	(-1.3,-1.3,0)	(-1.0,-1.0,-1.0)	(-1.6,0,0)	(-1.3,-0.63,0)	0.016
80 K	A_{1g}	D	(-1.4,0,0)	(-1.2,-0.30,0)	(-0.99,-0.99,-0.99)	(-1.7,0,0)	(-1.4,-0.69,0)	0.015
80 K	A_{1g}	D	(-1.4,0,0)	(-1.1,-1.1,0)	(-0.91,-0.91,-0.91)	(-1.5,0,0)	(-1.2,-0.60,0)	0.015

TABLE II. Displacements and relaxation energies for several defect systems. All the displacements and energies shown are for non- A_{1g} distortions. The displacements are in units 10^{-2} Å. The top values are Debye results, bottom modified Debye. In the case of KBr:OH^- and KCl:Li^+ where the low temperature elastic constants are known, results for both room temperature (RT) and low temperature (LT) are given.

System	Site					E (eV)
	100	110	111	200	210	
[100] Systems						
KBr:OH^-						
RT	(33,0,0)	(2.1,4.9,0)	(-2.3,1.2,1.2)	(7.1,0,0)	(4.4,0.55,0)	0.17
	(29,0,0)	(2.2,3.7,0)	(-0.3,0.16,0.16)	(7.6,0,0)	(4.4,1.2,0)	
LT	(39,0,0)	(2.4,5.7,0)	(-2.8,1.4,1.4)	(8.3,0,0)	(5.1,0.69,0)	0.24
	(34,0,0)	(2.4,4.3,0)	(-0.41,0.21,0.21)	(8.9,0,0)	(5.1,1.5,0)	
RbCl:OH^-	(24,0,0)	(1.5,3.6,0)	(-1.7,0.87,0.87)	(5.2,0,0)	(3.2,0.43,0)	0.082
	(21,0,0)	(1.5,2.7,0)	(-0.3,0.13,0.13)	(5.6,0,0)	(3.2,0.9,0)	
RbBr:OH^-	(42,0,0)	(2.5,6.3,0)	(-3.1,1.5,1.5)	(9.0,0,0)	(5.5,0.77,0)	0.21
	(37,0,0)	(2.6,4.8,0)	(-0.49,0.24,0.24)	(9.7,0,0)	(5.6,1.6,0)	
RbI:OH^-	(58,0,0)	(3.3,8.7,0)	(-4.3,2.1,2.1)	(12,0,0)	(7.5,1.1,0)	0.31
	(51,0,0)	(3.5,6.6,0)	(-0.72,0.36,0.36)	(13,0,0)	(7.6,2.3,0)	
[111] System						
KCl:Li^+						
RT	(0,1.3,1.3)	(1.3,1.3,-0.33)	(1.2,1.2,1.2)	(0,-0.03,-0.03)	(0.33,0.32,0.31)	0.0069
	(0,0.98,0.98)	(1.1,1.1,-0.18)	(1.1,1.1,1.1)	(0,0.14,0.14)	(0.39,0.30,0.20)	
LT	(0,1.3,1.3)	(1.3,1.3,-0.36)	(1.2,1.2,1.2)	(0,-0.03,-0.03)	(0.34,0.32,0.30)	0.0073
	(0,0.96,0.96)	(1.1,1.1,-0.20)	(1.1,1.1,1.1)	(0,0.13,0.13)	(0.40,0.29,0.19)	
[110] Systems						
NaBr:F^-	(2.9,0.54,0)	(1.3,1.3,0)	(-0.13,-0.13,0.4)	(0.61,0.05,0)	(0.42,0.27,0)	0.0092
	(2.5,0.44,0)	(1.0,1.0,0)	(0.02,0.02,0.05)	(0.64,0.09,0)	(0.43,0.27,0)	
RbCl:Ag^+	(18,1.1,0)	(7.6,7.6,0)	(-1.3,-1.3,2.8)	(3.9,0.12,0)	(2.9,1.5,0)	0.19
	(16,0.92,0)	(6.4,6.4,0)	(-0.15,-0.15,0.5)	(4.2,0.19,0)	(3.1,1.7,0)	
RbBr:Ag^+	(34,2.0,0)	(14,14,0)	(-2.4,-2.4,5.2)	(7.1,0.21,0)	(5.3,2.8,0)	0.54
	(29,1.6,0)	(12,12,0)	(-0.31,-0.31,1)	(7.7,0.33,0)	(5.7,3.1,0)	

VI. STRAIN FIELDS AND DEFECT INTERACTIONS

The displacement fields (22)–(25) and (30)–(32) can be differentiated with respect to the Cartesian components of lattice position to get expressions for elastic strain tensor components as a function of position relative to the defect. Interactions between defects can then be written down in analytic form using the strain components and the strain-defect in-

teraction expressions (2)–(5) suitably altered to include all possible defect orientations of the second defect.⁸ In this section only the modified Debye model will be used. We drop the tildes on Λ and K functions for convenience.

For the A_{1g} distortions

$$e_{xx} = -\frac{\gamma_0}{2\pi\rho} \left[\frac{1-3\xi^2}{R^3} \Lambda_2^l + \frac{\xi^2}{R^2} \Pi_2^l \right] \quad (36)$$

and cyclically for e_{yy} and e_{zz} . We have introduced the notation

$$\begin{aligned}\Pi_i^j &= \left[\frac{\tilde{\omega}_D}{c_j} \right] \left[\frac{d}{dg_j} \right] \Lambda_i^j(g_j) \\ &= (\tilde{\omega}_D/c_j^3) K_i'(g_j),\end{aligned}\quad (37)$$

where the K_j' are derivatives of the $K_i(g)$ given by

$$\begin{aligned}K_1'(g) &= \frac{1}{2}\pi \left[-\frac{2}{g} J_1(g) \right. \\ &\quad \left. + \frac{3\pi}{g^2} [J_1(g)H_0(g) - J_0(g)H_1(g)] \right] \\ &\sim (2\pi/g^3)^{1/2} \sin(g - \frac{1}{4}\pi),\end{aligned}\quad (38)$$

$$K_2'(g) = \frac{1}{2}\pi \left[\frac{2}{g} J_1(g) - J_0(g) \right] \sim (\pi/2g)^{1/2} \cos(g - \frac{1}{4}\pi),\quad (39)$$

$$\begin{aligned}e_{xx} &= (A_{100}/R^3)[3(3 - 24\xi^2 + 25\xi^4)(\Lambda_1^I - \Lambda_1^t) \\ &\quad - 2(1 - 12\xi^2 + 15\xi^4)\Lambda_2^I + 6(1 - 6\xi^2 + 5\xi^4)\Lambda_2^t] \\ &\quad + (A_{100}\xi^2/R^2)[3(3 - 5\xi^2)(\Pi_1^I - \Pi_1^t) + 2(3\xi^2 - 1)\Pi_2^I + 6(1 - \xi^2)\Pi_2^t],\end{aligned}\quad (40)$$

$$\begin{aligned}e_{yy} &= (A_{100}/R^3)[3(1 - 3\eta^2 - 5\xi^2 + 25\xi^2\eta^2)(\Lambda_1^I - \Lambda_1^t) \\ &\quad - 2(1 - 3\eta^2 - 3\xi^2 + 15\xi^2\eta^2)\Lambda_2^I + 6\xi^2(5\eta^2 - 1)\Lambda_2^t] \\ &\quad + (A_{100}\eta^2/R^2)[3(1 - 5\xi^2)(\Pi_1^I - \Pi_1^t) + 2(3\xi^2 - 1)\Pi_2^I - 6\xi^2\Pi_2^t],\end{aligned}\quad (41)$$

with e_{zz} being the same as e_{yy} if ξ replaces η there. The dilatation associated with this strain field is given by

$$e_{xx} + e_{yy} + e_{zz} = (1 - 3\xi^2)A_{100}[(6/R^3)(\Lambda_1^I - \Lambda_1^t + \Lambda_2^t) + (1/R^2)(3\Pi_1^I - 3\Pi_1^t - 2\Pi_2^t)].\quad (42)$$

This does not vanish but does average to zero over directions since $\langle \xi^2 \rangle = \frac{1}{3}$ so that the volume change associated with this E_g strain field is indeed zero. The elastic theory results follow in these and similar expressions if one sets Λ_i^j equal to $\pi/2c_j^2$ and all Π_i^j equal to zero.

The oscillating terms in the Λ and Π functions have an interesting consequence in the form of the strain components at large distances from the defect. Referring to the asymptotic forms of the Λ and Π functions [see (28), (29), (38), and (39)] one finds that the leading asymptotic terms for large R in (40)–(42) are those containing Π_2^t . These terms vanish as $R^{-5/2}$ for large R . In the elastic theory form of (40)–(42), with all the Π functions absent, the strains fall off as R^{-3} . Thus the effect of the oscillations arising from the Van Hove singularity at the modified Debye cutoff frequency is to make the range of defect-defect interactions somewhat greater

than that given by an elastic theory with no cutoff frequency. This is again reminiscent of the screening of a point charge by an electron gas in which the singularity in the dielectric function which arises because the sharpness of the Fermi surface produces static oscillations in the screening charge distribution and extends the range of interaction beyond what it is in theories which do not take such oscillations into account.

Neglecting the smaller longitudinal terms for simplicity, the leading terms of the asymptotic forms of the strain components (40) and (41) are

$$\begin{aligned}e_{xx} &\sim C(R/a)^{-5/2}\xi^2(1 - \xi^2)\cos(g_t - \frac{1}{4}\pi), \\ e_{yy} &\sim -C(R/a)^{-5/2}\xi^2\eta^2\cos(g_t - \frac{1}{4}\pi), \\ e_{zz} &\sim -C(R/a)^{-5/2}\xi^2\xi^2\cos(g_t - \frac{1}{4}\pi),\end{aligned}\quad (43)$$

where $C = (\gamma_1/c_{44}a^3)(3/2^5\pi^8)^{1/6}$ and

the asymptotic forms being those for large g . Note that for an A_{1g} defect the dilatation of the strain field does not vanish according to (36): $e_{xx} + e_{yy} + e_{zz} = -(\gamma_0/2\pi\rho R^2)\Pi_2^I$. In the elastic continuum limit it does vanish but our modified Debye theory produces this nonzero oscillating dilatation field. Consequently, interactions between A_{1g} defects are possible in this model although they do not occur in elastic continuum theory. As was seen in Sec. V for the only case in which γ_0 is known (KCl:OH⁻), the A_{1g} distortions are small compared with the E_g distortions. We will therefore omit the A_{1g} strains from further consideration in this section.

For [100] defect only e_{xx} , e_{yy} , e_{zz} play a role in defect interactions. The E_g strains arising from displacements (22)–(24) are given by

$g_t = \tilde{\omega}_D R / c_t \simeq (48\pi)^{1/3} (R/a)$. The spatial oscillations have a wavelength of the modified Debye transverse wavelength minimum. The asymptotic dilatation associated with (43) is zero so that the preferred orientation of a second $\langle 100 \rangle$ defect is determined by the maximum of e_{xx} , e_{yy} , e_{zz} according to (2). This is determined by the sign of the cosine factor in (43). For a given distance R , except for $\xi = 1$ or 0 , all the second-defect-preferred orientations are either with the x direction or in the y, z direction (degenerate) depending on the sign of the cosine factor. These asymptotic strains can be compared with those of elastic theory which are, again neglecting the longitudinal terms,

$$\begin{aligned} e_{xx} &\sim -C'(1 - 12\xi^2 + 15\xi^4)(R/a)^{-3}, \\ e_{yy} &\sim -C'(1 - 3\eta^2 - 3\xi^2 + 15\xi^2\eta^2)(R/a)^{-3}, \\ e_{zz} &\sim -C'(1 - 3\xi^2 - 3\xi^2 + 15\xi^2\xi^2)(R/a)^{-3}, \end{aligned} \quad (44)$$

where $C' = (\gamma_1/c_{44}a^3)/8\pi$ which is about $\frac{1}{3}$ the C of (43).

The critical concentration c_e at which elastic dipole defect interactions begin to be important for $\langle 100 \rangle$ defects occurs when the average distance between defects is such that $\gamma_1 e_{xx}$ is equal to the matrix element Δ associated with nearest-neighbor tunneling of the defect. Strains (43) and (44) give different estimates of this concentration. For KCl:OH^- for which $\alpha_1 = 5.8 \text{ \AA}^3$, $\Delta = 0.17 \text{ cm}^{-1}$, c_e (mole fraction of KOH in KCl) estimated from the modified Debye asymptotic strains (43) is 1.9×10^{-5} while that estimated from the elastic continuum asymptotic strains (44) is 4.3×10^{-4} , 20 times greater than the modified Debye model estimate. Unfortunately, accurate information about the critical concentration in KCl:OH^- is not available.

Of course OH^- is also an electric dipole (p). The critical concentration for electric dipole interactions is $c_d \sim \epsilon \Delta a^3 / p^2$. ϵ is the static dielectric constant.

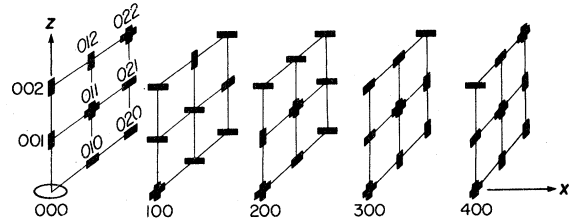


FIG. 2. Preferred orientations of a second $\langle 100 \rangle$ defect in the strain field of a $[100]$ -oriented elastic dipole at the 000 site according to Eqs. (2), (40), and (41) for the case of KCl:OH^- .

The electric dipole of OH^- in KCl is $0.9e \text{ \AA}$ so that for KCl:OH^- $c_d \sim 2.4 \times 10^{-4}$. The elastic continuum estimate of the elastic dipole interaction critical concentration would suggest that electric dipole interactions would very slightly dominate but the modified Debye model estimate of c_e suggests that this may not in fact be the case.

Ignoring the electric dipole interactions just for a moment, Fig. 2 shows the preferred orientations of a second OH^- in the immediate vicinity of a $[100]$ -oriented OH^- defect in KCl based on the elastic dipole interaction alone using (2), and (40) and (41). It can be seen that the preferred orientation pattern is quite complicated even close to the central defect. Far from the defect where the asymptotic strains vary rapidly with distance from the central defect the pattern would be even more chaotic, although the angular dependence of preferred orientation for a given distance is, as we have seen, in the case of $\langle 100 \rangle$ defects essentially absent. Paraelastic defect interactions seem to lend themselves to an orientational glass state.¹⁸

A more favorable case for domination of defect interactions by elastic dipole interactions is KCl:CN^- where the electric dipole is small $p \sim 0.1e \text{ \AA}$. This is a $\langle 111 \rangle$ system.

Off-diagonal strain components for a $\langle 111 \rangle$ defect are given by

$$\begin{aligned} e_{xy} = & \frac{A_{111}}{R^3} \{ [2(\Lambda_2^l - \Lambda_2^t) - 5(\Lambda_2^l)] [-6\xi\eta(\xi\eta + \eta\xi + \xi\xi) + \xi(\xi + \eta)(1 - 2\xi^2) \\ & + \eta(\xi + \xi)(1 - 2\eta^2) - 2\xi\eta\xi(\xi + \eta)] \\ & + (\Lambda_1^l - \Lambda_1^t + \Lambda_2^t) [2 - 3\xi^2 - 3\eta^2 - 3\xi(\eta + \xi)] \} \\ & + \frac{A_{111}}{R^2} \{ 2[2(\Pi_2^l - \Pi_2^t) - 5(\Pi_1^l - \Pi_1^t)] \xi\eta(\xi\eta + \eta\xi + \xi\xi) \\ & + (\Pi_1^l - \Pi_1^t + \Pi_2^t) [\eta(\xi + \eta) + \xi(\xi + \xi)] \} \end{aligned} \quad (45)$$

and cyclically for e_{yz} and e_{zx} . Asymptotically, for large R , keeping only the transverse terms,

$$e_{xy} \sim \frac{3}{4} \frac{\gamma_2}{c_{44}a^3} \left(\frac{3}{2^5\pi^8} \right)^{1/6} \left(\frac{R}{a} \right)^{-5/2} \cos(g_t - \frac{1}{4}\pi) [1 - \zeta^2 + \eta\zeta + \zeta\xi - 4\xi\eta(\xi\eta + \eta\zeta + \zeta\xi)] \quad (46)$$

and cyclically.

Using (46) one can estimate the critical density for elastic dipole interactions in KCl:CN^- ($\gamma_2 = 5.1 \times 10^{-13}$ erg) as $c_e \sim 2.3 \times 10^{-3}$. The electric dipole moment interactions produce a critical density $c_d \sim 7.8 \times 10^{-2}$. This is a case in which the elastic dipoles most assuredly dominate. Holuj and Bridges¹⁹ have observed interaction effects in paraelectric resonance experiments at a concentration of 10^{-3} .

Preferred orientations of a second $\langle 111 \rangle$ defect asymptotically far from the central $[111]$ defect calculated from (46) and (3) with its other forms are given in Figs. 3 and 4 for negative and positive $\cos(g_t - \frac{1}{4}\pi)$ in (46). For a negative cosine factor most of the sites have a preferred orientation parallel to the central $[111]$ defect except for a few sites in the $[111]$ direction and sites near the great circle

on the sphere which has a plane perpendicular to $[111]$. For a positive cosine factor the pattern is more complicated. In this case, however, the numbers of sites with preferred $[\bar{1}11]$, $[1\bar{1}1]$, and $[11\bar{1}]$ orientations are all the same. There are no sites with preferred $[111]$ orientations for a positive cosine factor. In the $[111]$ defect case with positive cosine factor, unlike the $[100]$ defect case, there is a marked dependence of preferred orientation on direction of the defect site as well as a rapidly oscillating dependence on the distance to this site.

Strain component expressions around a $[110]$ defect are readily deduced from (31) and (32) but the rather lengthy expressions are not given here. The preferred orientations of an asymptotically distant second $\langle 110 \rangle$ defect varies markedly not only with distance but also with direction.

Note added. In a theoretical investigation of ul-

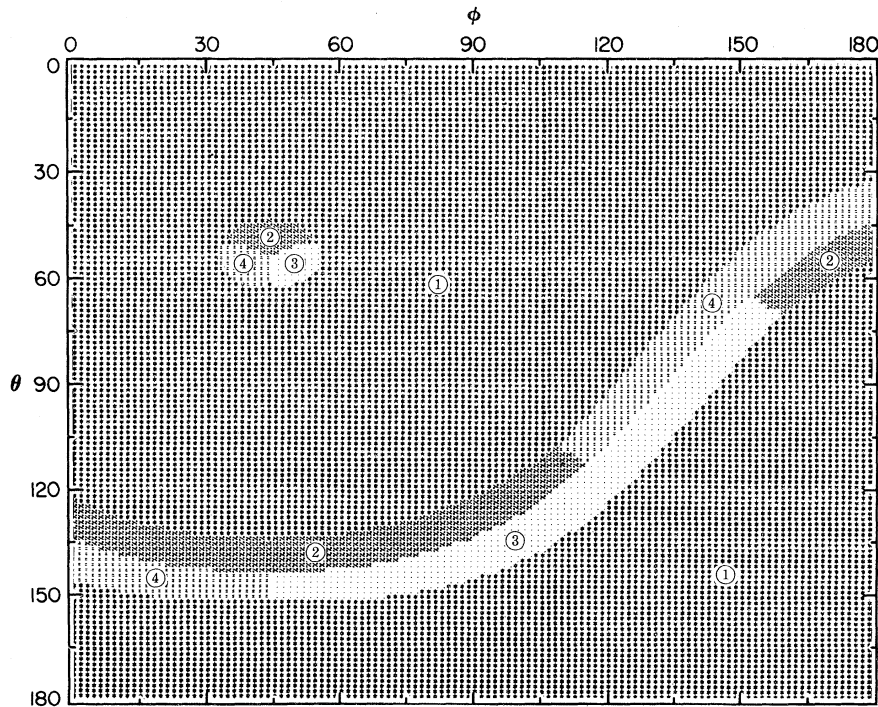


FIG. 3. Preferred orientations of a second $\langle 111 \rangle$ defect in the asymptotic strain field of a $[111]$ -oriented defect at the origin. The distance from the origin is such that $\cos(g_t - \frac{1}{4}\pi)$ in Eq. (46) is negative. The plot is a mercator projection of the spherical surface surrounding the origin. The projection of the $[111]$ direction occurs at $\theta = 54.7^\circ$ and $\phi = 45^\circ$. The regions labeled 1 have preferred $[111]$ direction. Those labeled 2, 3, and 4 have preferred $[1\bar{1}1]$, $[\bar{1}11]$, and $[\bar{1}\bar{1}1]$ directions. The parameters used are those for KCl:Li^+ .

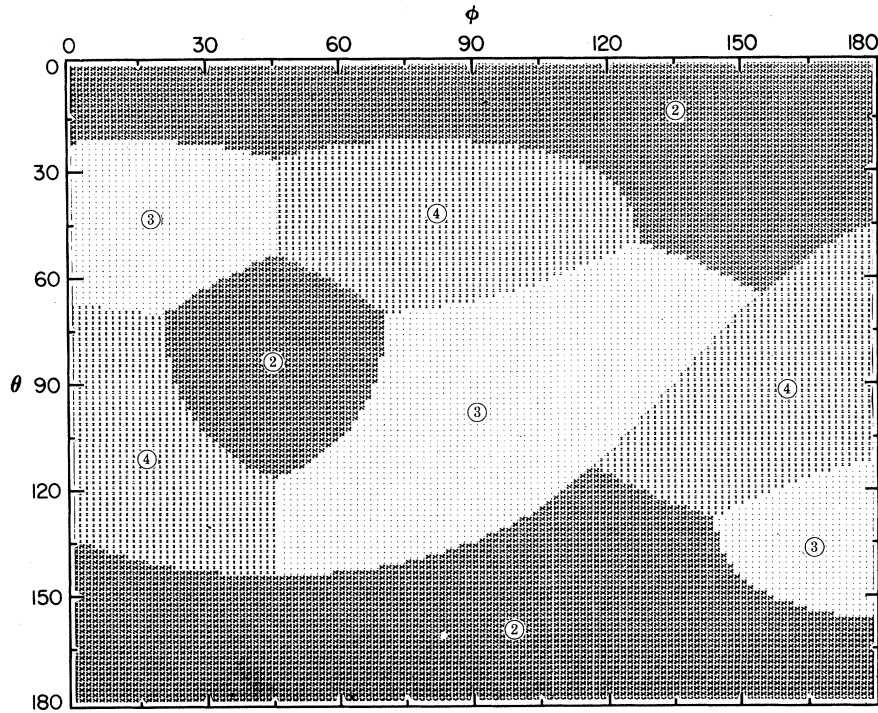


FIG 4. The same as Fig. 3 but for positive $\cos (g_t - \frac{1}{4} \pi)$ in (46).

trasonic attenuation in glasses Joffrin and Levelut²⁰ have done a Debye calculation similar to the one described here. They have not investigated the modified Debye case.

ACKNOWLEDGMENTS

This work was done with the support of NSF Grant No. DMR 77-25773. I wish to thank F. Lüty, J. Ball, and H. Monkhorst for some helpful discussions.

APPENDIX

The simpler of the two integrals \tilde{K}_1 and \tilde{K}_2 is the latter:

$$\begin{aligned} \tilde{K}_2(g) &= \int_0^1 \frac{dy}{y} (1 - y^2)^{1/2} \text{siny} \\ &\quad - 2g \int_0^1 dy (1 - y^2)^{1/2} \text{cosgy} \\ &= \int_0^1 dy (1 - y^2)^{1/2} \int_0^g dt \text{cosyt} - \pi J_1(g) \\ &= \frac{\pi}{2} \int_0^g dt J_1(t)/t - \frac{\pi}{2} J_1(g), \end{aligned}$$

where Ref. 21 (3.752.2), has been used. The integral involving the Bessel function is given in Ref. 21 (6.561.13) as corrected by referring to the source given there and we get

$$\begin{aligned} \tilde{K}_2 &= \frac{1}{2} \pi [1 - gJ_1(g)S_{-2,0}(g) \\ &\quad - gJ_0(g)S_{-1,1}(g) - J_1(g)]. \end{aligned}$$

The $S_{\mu\nu}(g)$ are Lommel functions which can be expressed in terms of Struve functions and Bessel functions by use of identities given in Ref. 22. In getting (29) we have also used the Wronskian identity given in Ref. 23 (9.1.16).

The integral

$$\tilde{K}_1(g) = 2g \int_0^1 dy (1 - y^2)^{1/2} j_2(gy)$$

can be performed by first using an integral representation of j_2 , Poisson's integral, given in Ref. 22 (10.1.4). $\tilde{K}_1(g)$ then yields to the same methods as were used for $\tilde{K}_1(g)$. The asymptotic forms in (28) and (29) can be found by use of Ref. 23 (12.1.30).

- ¹R. Pirc, B. Zeks, and P. Gosar, *J. Phys. Chem. Solids* **27**, 1219 (1966).
- ²H. B. Shore and L. M. Sander, *Phys. Rev. B* **12**, 1546 (1975).
- ³D. L. Tonks and B. G. Dick, *Phys. Rev. B* **19**, 1136 (1979).
- ⁴D. L. Tonks and B. G. Dick, *Phys. Rev. B* **19**, 1149 (1979).
- ⁵R. Pirc and P. Gosar, *Phys. Kondens. Mater.* **9**, 377 (1969).
- ⁶L. M. Sander and H. B. Shore, *Phys. Rev. B* **3**, 1472 (1971).
- ⁷A brief account of this formalism appears in B. G. Dick, *Phys. Rev. B* **16**, 3359 (1977).
- ⁸F. Bridges, *Crit. Rev. Solid State Sci.* **5**, 1 (1975), Table AIII-2.
- ⁹W. Brenig and W. Götze, *Z. Phys.* **217**, 188 (1968).
- ¹⁰A. C. Hearn, *REDUCE 2 Users Manual* (University of Utah, 1973, unpublished).
- ¹¹J. Friedel, *Philos. Mag.* **43**, 153 (1952).
- ¹²H. Paus and F. Lüty, *Phys. Status Solidi* **12**, 341 (1965).
- ¹³A. S. Nowick and W. R. Heller, *Adv. Phys.* **12**, 251 (1963).
- ¹⁴M. J. Lighthill, *Introduction to Fourier Analysis and Generalized Functions* (Cambridge University Press, Cambridge, 1960).
- ¹⁵H. B. Rosenstock, *Phys. Rev.* **97**, 290 (1955).
- ¹⁶Y. L. Luke, *Algorithms for Computation of Mathematical Functions* (Academic, New York, 1977).
- ¹⁷H. B. Huntington, in *Solid State Physics*, edited by F. Seitz and D. Turnbull (Academic, New York 1968), Vol. 7.
- ¹⁸B. Fisher and M. W. Klein, *Phys. Rev. Lett.* **43**, 289 (1979).
- ¹⁹F. Holuj and F. Bridges, *Phys. Rev. B* **20**, 3578 (1979).
- ²⁰J. Joffrin and A. Levelut, *J. Phys. (Paris)* **36**, 811 (1975).
- ²¹I. S. Gradshteyn and I. M. Ryzhik, *Table of Integrals, Series and Products* (Academic, New York, 1965).
- ²²W. Magnus, F. Oberhettinger, and R. P. Soni, *Formulas and Theorems for the Special Functions of Mathematical Physics* (Springer, New York, 1966).
- ²³*Handbook of Mathematical Functions*, U.S. Natl. Bur. Stand. (Appl. Math. Ser. No. 55), edited by M. Abramowitz and I. A. Stegun (U.S. GPO, Washington, D.C., 1964).